

Electric Motor HILS System Using Numerical Stabilization Technique for Simulating Nonlinear Coupled System

Kei MORITA*¹

*¹ Production Systems Research Laboratory, Technical Development Group

This paper introduces a stabilization technique of nonlinear coupled analysis for hydraulic excavators, in which a rigid body system and a hydraulic system are coupled. Also introduced is a "Hardware-In-the-Loop Simulation (HILS)" for electric motors, in which the above technique is exploited. The rigid body system consists of a rotating element and a linear motion element, and the stabilization technique converts the motion of the rotating element into linear motion, enabling the motion of both the systems to be described in an ordinary differential equation without introducing any constraint conditions for the rigid bodies. This enables a coupled analysis with one motion equation that shares the state quantities of both the systems, thus improving the stability of the numerical analysis. This technique has been used to simulate in real-time the actual load acting on the electric motor, which has been reproduced on a motor-load testing apparatus and has realized an electric motor HILS system.

Introduction

The requirements on greenhouse gas emission reduction have become more stringent to suppress global warming, and improvement in fuel economy is now an important issue also for hydraulic excavators. In an effort to improve the fuel economy, hybrid systems have been in development to drive upper slewing bodies by electric motors so as to utilize the energy of their deceleration effectively.^{1), 2)} The development of hybrid systems requires fully understanding the characteristics of their electric motors and then optimizing their control systems. Hardware In the Loop Simulation (HILS)^{note 1)} offers an effective means for improving development efficiency. A hydraulic excavator, however, calls for non-linear analysis, in which a "hydraulic system," showing strong non-linearity, and a "rigid body system," including link mechanisms such as booms, are coupled. This presents a challenge in ensuring the stability of the numerical analysis.

^{note 1)} A technology for evaluating the performance and quality of hardware to be developed by connecting and running the hardware to be developed by simulating in real-time the entire system other than said hardware.

Meanwhile, HILS is used for the development of engines, transmissions, electronic control units (ECUs), etc., in the field of automobiles³⁾ and for virtual testing on running stability, among other things, in the field of railroad equipment,⁴⁾ thus contributing greatly to the improvement of development efficiency, performance, and quality. So far, however, almost no HILS system has been reported as established, in which real-time calculation is carried out using an analysis model in which a rigid body system and hydraulic system are coupled together, as in the case of hydraulic excavators.

This paper describes a technology for improving the numerical stability of "SINDYS," a simulation program for non-linear systems, including a hydraulic system coupled with a linkage mechanism on the basis of a modeling technique for converting the movement of a rigid body system from rotating element motion to linear element motion.⁵⁾ As also introduced in this paper, this stabilization technology has been adapted for an HILS system for electric motors,⁶⁾ in which the system calculates the load acting on an electric motor in real time during work and reproduces it on an apparatus for testing the load acting on the electric motor. The target is a hybrid system with an upper slewing body rotationally driven by an electric motor.

1. Coupled analysis theory for rigid body-hydraulic system

1.1 Analysis model for hydraulic excavators

Fig. 1 depicts the linkage model of a hydraulic excavator. The attachments on this hydraulic excavator consist of a boom, arm, and bucket, which are coupled with the upper slewing body. Each linkage of the boom, arm, and bucket is independently driven by the corresponding, elongating/contracting hydraulic cylinder. The upper slewing body is driven by an electric motor via a slewing bearing and reduction gears and makes a slewing movement involving the attachments. The above configuration is modeled using the formulation of a rigid body system which will be described later.

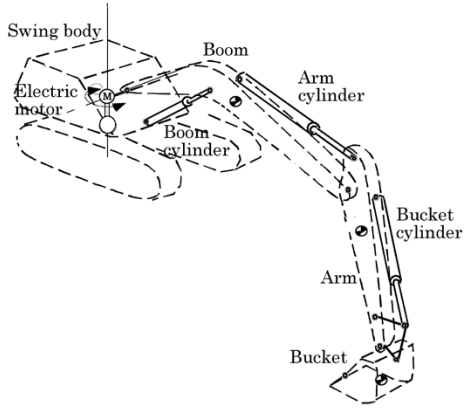


Fig. 1 Linkage model of hydraulic excavator

Fig. 2 shows the hydraulic system for driving the attachments. This system comprises two hydraulic pumps driven by the engine to supply hydraulic pressure, in which control valves are operated in accordance with the levers manipulated by an operator. This system thus changes the opening area to each branch piping and controls the flow rate of hydraulic oil supplied from the pump to the hydraulic cylinder.

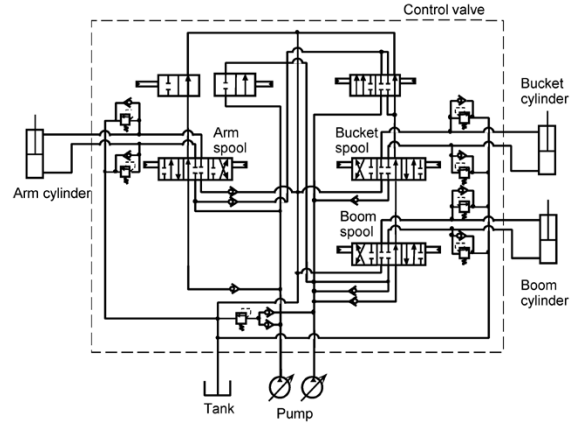


Fig. 2 Hydraulic system of hydraulic excavator

1.2 Motion equation of coupled system⁵⁾

The coupled analysis of a rigid body system and hydraulic system involves the analysis of a non-linear motion equation (Equation (1)) consisting of the superimposition of MCK type motion equations in each system:

$$M\ddot{\mathbf{q}}_{n+1} + C\dot{\mathbf{q}}_{n+1} + K\mathbf{q}_{n+1} = \mathbf{f}_{n+1} - \bar{\mathbf{f}}_n \dots \dots \dots (1)$$

wherein \mathbf{q}_{n+1} is a vector representing the state quantities such as the displacement and rotation angle at time t_{n+1} in a rigid body system, and such as the flow rate product (integral of volumetric flow rate) in a hydraulic system. \mathbf{M} , \mathbf{C} , and \mathbf{K} represent the mass, attenuation, and stiffness matrices linearized at time t_n , respectively, and \mathbf{f}_{n+1} is the external force at time t_{n+1} . The term $\bar{\mathbf{f}}_n$ is the external force corrected by linearizing the non-linear elemental force at each time step. As shown in Fig. 3, the stiffness element can be expressed as $K\mathbf{q}_{n+1} = \mathbf{f}_{n+1} - \bar{\mathbf{f}}_n$ by introducing the corrected external force. Here, $\bar{\mathbf{f}}_n = \mathbf{f}_n - K\mathbf{q}_n$. The same applies to the mass and attenuation elements. The time integration employs the Newmark β method ($\beta = 1/4$).

1.3 Formulation of rigid body system⁵⁾

As the model of the slewing body of a hydraulic excavator, a rigid body linkage model as shown in Fig. 4 is considered. This model consists of four rigid bodies. Body 0 only rotates around the y-axis

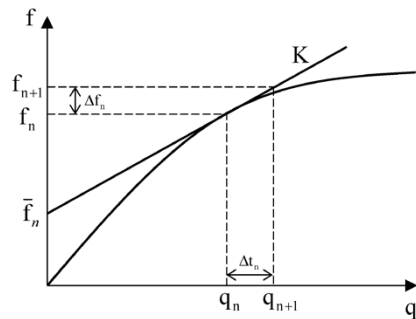


Fig. 3 Corrected external force by linearization

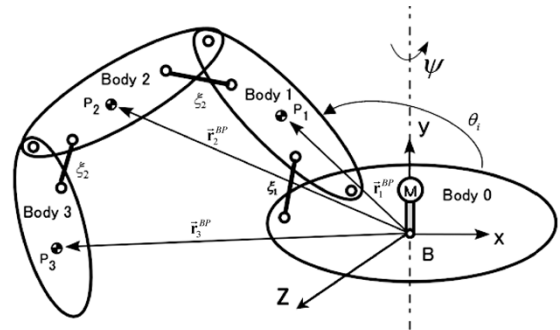


Fig. 4 Rigid body linkage model

(rotational angle, ψ) without moving translationally. Body 1 is constrained to body 0 by a pin joint, is driven translationally by the linear motion element between body 0 and body 1 (cylinder displacement, ξ_1), and rotates around the z-axis (rotational angle, θ_1). The same applies to body 2 and body 3. Bodies 1 to 3 move (rotation angle, ψ) together as a result of body 0 rotating around the y-axis. In this way, in the rigid body system, each rigid body's motion at the position of its center of gravity (P_i ($i = 1$ to 3)) can be expressed by the rotating motion and translational drive by linear motion elements.

On the other hand, in the hydraulic system described in Subsection 1.4, the motions of its linear elements such as a hydraulic cylinder are expressed by their translational displacements to express their motions in one dimensional state quantities.

Therefore, in the case of the coupled analysis of a rigid body system and hydraulic system, expressing the rotational motion of the rigid body system in terms of the motion of the linear motion element allows the motion of both the systems to be expressed by an ordinary differential equation without introducing any constraint conditions. This eliminates the need for modeling with separate pieces of software and calculating, while changing the state quantities for each time step, when the coupled analysis of each system is carried out. As a result, it has become possible to carry out a coupled analysis with only one piece of software, which improves stability in the numerical analyses.

Now, in order to convert the motion of a rigid body system as shown in Fig. 4 from the motion of the rotating element to the motion of the linear motion element, the position of the center of gravity of each body is described by the rotational angle around z-axis and, in addition, the rotation angle around the z-axis is described by the cylinder's displacement so as to express the motion of the linear motion element.

First, the motion equation for the point P_i and slewing axis is that for the rigid body system and is given by Equation (2):

$$\mathbf{M}_e \ddot{\mathbf{w}} = \mathbf{f}_e \quad \dots\dots\dots (2)$$

wherein \mathbf{M}_e is an inertia matrix consisting of the mass of point P_i and inertia moment around the y-axis of the body 0, and \mathbf{f}_e is an external force vector. The term $\ddot{\mathbf{w}}$ represents an acceleration matrix, $\ddot{\mathbf{w}} = [\ddot{\mathbf{r}}_1^T \ \ddot{\mathbf{r}}_2^T \ \ddot{\mathbf{r}}_3^T \ \ddot{\psi}]^T$, $\ddot{\mathbf{r}}_i = [\ddot{x}_i \ \ddot{y}_i \ \ddot{z}_i]$, in which $\ddot{\mathbf{r}}_i$ is the acceleration of the point P_i seen from point B, and $\ddot{\psi}$ is the angular acceleration of slewing.

Next, assuming that the angle of bodies 1 to 3 around the z-axis of point B is θ_i , the acceleration matrix $\ddot{\mathbf{w}}$ is given by Equation (3) using the coordinates transformation matrices \mathbf{G}_{11} and \mathbf{G}_{12} .

$$\ddot{\mathbf{w}} = \mathbf{G}_{11} \ddot{\mathbf{q}}_\theta + \mathbf{G}_{12} \ddot{\mathbf{q}}_\xi \quad \dots\dots\dots (3)$$

wherein $\ddot{\mathbf{q}}_\theta = [\ddot{\theta}_1 \ \ddot{\theta}_2 \ \ddot{\theta}_3 \ \ddot{\psi}]^T$, $\ddot{\mathbf{q}}_\xi = [\ddot{\xi}_1 \ \ddot{\xi}_2 \ \ddot{\xi}_3 \ \ddot{\psi}]^T$.

In addition, using each cylinder displacement ξ_i instead of angle θ_i gives the relation of Equation (4).

$$\ddot{\mathbf{q}}_\theta = \mathbf{G}_{23} \ddot{\mathbf{q}}_\xi \quad \dots\dots\dots (4)$$

wherein $\ddot{\mathbf{q}}_\xi = [\ddot{\xi}_1 \ \ddot{\xi}_2 \ \ddot{\xi}_3 \ \ddot{\psi}]^T$. Moreover, differentiating Equation (4) gives the relationship between $\ddot{\mathbf{q}}_\theta$ and $\dot{\mathbf{q}}_\xi$.

$$\ddot{\mathbf{q}}_\theta = \mathbf{G}_{23} \dot{\mathbf{q}}_\xi + \mathbf{G}_{23} \ddot{\mathbf{q}}_\xi \quad \dots\dots\dots (5)$$

From the above, Equation (6) is obtained by substituting Equations (3), (4), and (5) for Equation (2).

$$\mathbf{M}_\xi \ddot{\mathbf{q}}_\xi + \mathbf{C}_\xi \dot{\mathbf{q}}_\xi = \mathbf{Q}_\xi \quad \dots\dots\dots (6)$$

This allows the motion of each body to be described by the motion of a linear motion element.

1.4 Analysis theory of hydraulic system⁷⁾

The hydraulic system shown in Fig. 2 is modeled. The following explains an example of a piping element, which is the basic element. For a piping element, it is necessary to express the compressibility and branching of hydraulic fluid in piping, and in the case of a piping element with three ports, the element motion equation described in terms of the flow rate product q_i of each port is given by Equation (7).

$$\rho \begin{bmatrix} l_1/A_1 & 0 & 0 \\ 0 & l_2/A_2 & 0 \\ 0 & 0 & l_3/A_3 \end{bmatrix} \begin{bmatrix} \dot{q}_1 \\ \dot{q}_2 \\ \dot{q}_3 \end{bmatrix} + \frac{\kappa}{V_0} \begin{bmatrix} \lambda_1^2 & \lambda_1 \lambda_2 & \lambda_1 \lambda_3 \\ \lambda_1 \lambda_2 & \lambda_2^2 & \lambda_2 \lambda_3 \\ \lambda_1 \lambda_3 & \lambda_2 \lambda_3 & \lambda_3^2 \end{bmatrix} \begin{bmatrix} q_1 \\ q_2 \\ q_3 \end{bmatrix} = \begin{bmatrix} 0 \\ 0 \\ 0 \end{bmatrix} \quad \dots (7)$$

This coefficient matrix constitutes the element mass matrix \mathbf{M}_e and element stiffness matrix \mathbf{K}_e , as expressed by Equation (8).

$$\mathbf{M}_e = \rho \begin{bmatrix} l_1/A_1 & 0 & 0 \\ 0 & l_2/A_2 & 0 \\ 0 & 0 & l_3/A_3 \end{bmatrix}, \mathbf{K}_e = \frac{\kappa}{V_0} \begin{bmatrix} \lambda_1^2 & \lambda_1 \lambda_2 & \lambda_1 \lambda_3 \\ \lambda_1 \lambda_2 & \lambda_2^2 & \lambda_2 \lambda_3 \\ \lambda_1 \lambda_3 & \lambda_2 \lambda_3 & \lambda_3^2 \end{bmatrix} \quad \dots\dots (8)$$

wherein ρ , l , A are hydraulic oil density, piping length, and cross-section, respectively; and κ , V_0 , λ are the bulk modulus, volume in the piping, and the coordinate transformation coefficient showing the inflow/outflow at each port of the hydraulic fluid, respectively.

For piping pressure loss, the relationship between the pressure difference Δp and volume flow \dot{q} is defined by Equation (9).

$$\Delta p = c_1 \dot{q}^{1.75} + c_2 \dot{q}^2 \quad \dots\dots\dots (9)$$

Here, the first term of the right-hand side shows the pressure loss characteristics of a straight pipe and the second term shows the pressure loss characteristics for cases with rapid expansion/contraction, vent, elbows, and so on.

The coefficient c_1 is determined from various parameters such as the length of the straight pipe and the pipe diameter; c_2 is a coefficient determined by factors such as rapid expansion/contraction, vent, and elbows. A corrected external force is introduced into Equation (9) for the linearization at time t_n .

In addition, for a check valve for direction control and relief valve for pressure control, the relationship between pressure difference Δp and flow rate \dot{q} is defined as an attenuation element with piecewise-linear characteristics. Likewise, a corrected external force is introduced into each of these for the linearization at time t_n .

In this way, the motion of the hydraulic system

can be described by a motion equation (Equation (10)).

$$M_e \ddot{q}_{n+1} + C \dot{q}_{n+1} + K_e q_{n+1} = f_{n+1} - \bar{f}_n \quad \dots\dots\dots (10)$$

2. Digging operation simulation of hydraulic excavator

The modeling technique described in Section 1 was used for the dynamic simulation of the attachment in the digging operation of the hydraulic excavator. This section shows the validity of this technique by comparing the simulation results with the actual measurement results. In addition, the numerical stability of this technique is shown by solving the motion equations of the rigid body system and hydraulic system independently as a conventional technique to make a comparison with the results calculated by co-simulation, in which the state quantities are replaced at every time step.

2.1 Results of dynamic simulation for digging operation

The hydraulic excavator's digging operation was analyzed for one cycle and compared with actual measurement results. The digging operation is roughly classified into four working modes, i.e., drilling, boom raising/slewing, dumping, and boom lowering/slewing, in which all the actuators except for the traveling actuator are working. In this analysis, the lever input employed actually measured the operation lever pattern (pilot pressure) of each actuator, and the slewing speed employed measured speed as the target value. The digging reaction force from the ground was defined as a concentrated load on the bucket node and was given by a function defining the direction and the size in accordance with the angle and locus of the bucket. **Fig. 5** compares the result of the measurement of the cylinder stroke with the analysis result. The calculation time steps of the analysis were 1 ms and 10 ms. The comparison shows that the analysis results respectively agree with the experimental results by $\pm 4\%$ or less, verifying the validity of this analysis technique.

2.2 Evaluating numerical stability of analysis technique

In order to ensure the simultaneity of the analysis to be applied to HILS, it is important to ensure its numerical stability even when the time step width is increased. The numerical stability of this analysis technique is shown in **Fig. 6**, in which the analysis

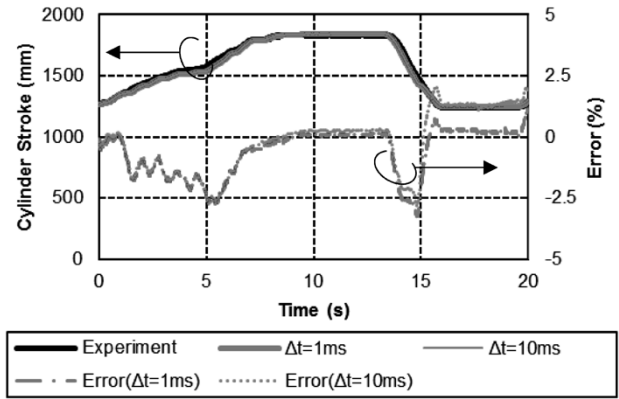


Fig. 5 Evaluation of numerical instability in digging operation ($\Delta t = 1 \text{ ms}, 10 \text{ ms}$)

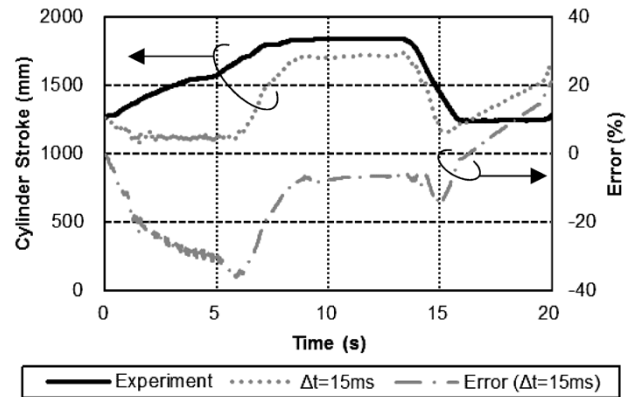


Fig. 6 Evaluation of numerical instability in digging operation ($\Delta t = 15 \text{ ms}$)

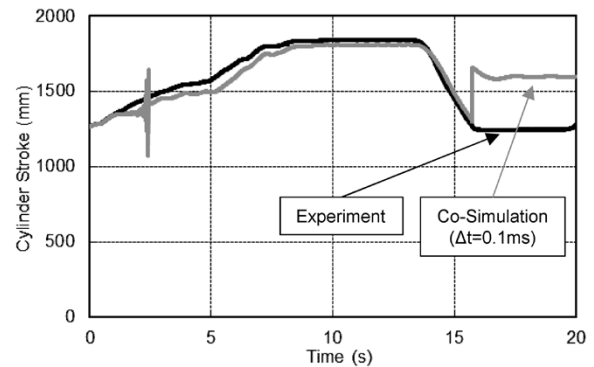


Fig. 7 Comparison of experimental and co-simulation technique results

was performed with a calculation time step of 15 ms. The fact that the time step of 15 ms results in a significant error deviating from the experimental results (approximately 35%) shows that an equivalent level of accuracy can be secured up to the time step of 10 ms.

On the other hand, in the conventional technique, the motion equations were solved for the rigid body system and the hydraulic system independently, and the state quantities are changed for each time step to carry out co-simulation. The results are shown in **Fig. 7**. It is shown that the accuracy is not sufficient

even when the time step is 0.1 ms.

As shown above, this stabilization technique improves the numerical stability of the coupled analysis of a rigid body system and hydraulic system, enabling the application of the coupled analysis to HILS.

3. HILS system for electric motors

The following describes an example of this stabilization technique used for a hybrid system where the upper slewing body is rotationally driven by an electric motor, and introduces an electric motor HILS system, in which the load acting on the electric motor during actual work is calculated in real time and reproduced on an electric-motor-load testing apparatus.

Fig. 8 shows the configuration of the electric-motor-load testing apparatus. This apparatus comprises an electric motor, dynamo, resolver, torque meter, bearing, electric motor, inverter (INV), control PC, and computation PC.

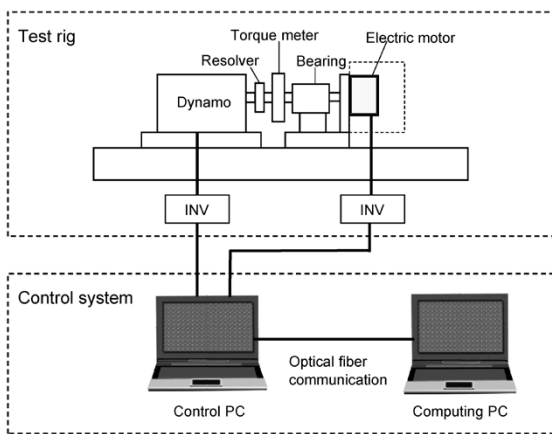


Fig. 8 Apparatus of load test for electric motor

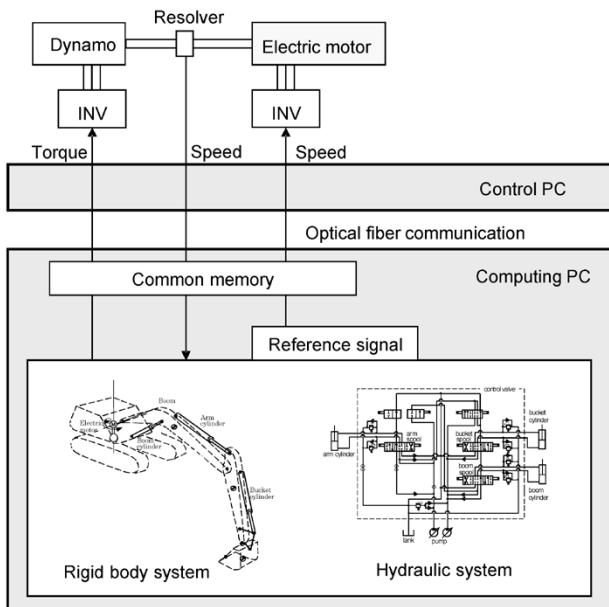


Fig. 9 Schematics of HILS system for electric motor

torque meter, control PC, and computation PC. In the computation PC, the digging operation of the hydraulic excavator is simulated on the basis of the coupled analysis model of a rigid body system and hydraulic system, described in the previous chapter, in which the slewing torque is derived from the operation input and is made to act on the electric motor by a dynamo as the load for the electric motor.

The mechanism of the electric-motor HILS system is explained on the basis of the signal flow among the components shown in Fig. 9. First, the target signal of an operation input for slewing speed is sent from the computation PC to the inverter of the electric motor via the control PC, and the rotation speed of the electric motor is controlled on the basis of the target signal. The actual RPM of the electric motor is detected by the resolver, and the load torque acting on the electric motor is calculated in the computation PC in real time in accordance with the RPM and is sent to the control PC.

The dynamo is torque-controlled by the control PC on the basis of the load torque.

4. Evaluation of dynamic simulation and electric motor HILS for hybrid system

The analysis model described in Section 2 is adapted for the electric motor HILS system to carry out the HILS evaluation of the electric motor during the digging operation of the hydraulic excavator. In this section, the analysis model of a hydraulic excavator with electric slewing function is prepared first to be compared with the actual work result to verify the validity of the analysis model. Next, HILS testing using the electric-motor-load testing apparatus is performed for comparison with the result of the analysis model so as to verify the validity of the electric motor HILS system.

4.1 Analysis model for electric motor⁶⁾

The electric motor is a permanent magnet type three-phase synchronous electric motor, and the equivalent circuit of the q-axis, among the equivalent direct current circuits represented by d-q coordinates (rotating coordinates rotating synchronously with rotating magnetic field), is modeled. The equivalent circuit of the q-axis in the electric motor model, taking into account the inverter loss, is shown in Fig.10. Assuming that the state quantities of the electric motor have 3 degrees of freedom, namely, the q-axis equivalent current \hat{q}_q , q-axis equivalent iron loss current \hat{q}_{cq} , and electric motor RPM $\hat{\theta}_m$, the electric circuit equation⁸⁾ and the motion equation are given by Equation (11).

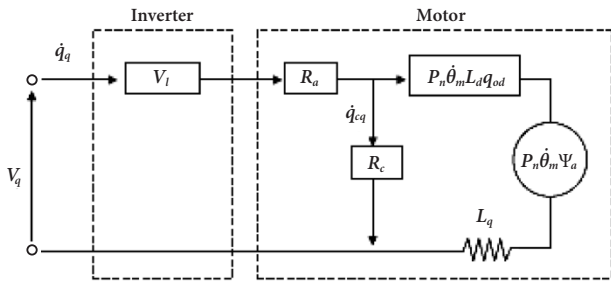


Fig.10 Equivalent circuit of q-axis in electric motor model

$$\begin{aligned}
 L_q \ddot{q}_q - L_q \ddot{q}_{cq} + R_a \dot{q}_q + P_n \dot{\theta}_m (L_d \dot{q}_{od} + \Psi_a) &= V_q - V_i \\
 L_q \ddot{q}_{cq} - L_q \ddot{q}_q + R_c \dot{q}_{cq} - P_n \dot{\theta}_m (L_d \dot{q}_{od} + \Psi_a) &= 0 \quad \dots\dots\dots (11) \\
 J_m \ddot{\theta}_m + C_m \dot{\theta}_m &= T
 \end{aligned}$$

wherein L_d and L_q are the d-axis and q-axis inductance, respectively, of the electric motor, R_a is the electric motor winding resistance, R_c is the electric motor equivalent iron loss resistance, P_n is the number of the pole pairs, Ψ_a is the interlinkage magnetic flux, V_q is the equivalent circuit voltage of the q-axis, V_i is the inverter equivalent loss voltage drop, J_m is the electric motor inertia moment, C_m is the electric motor viscosity resistance, and T is the electric motor torque. It should be noted that the equivalent circuit current \dot{q}_d of the d-axis is considered to be ideally controlled for its electric current phase, and Equation (12) is used.

$$\dot{q}_d = -\dot{q}_q \tan \beta \quad \dots\dots\dots (12)$$

wherein β is the phase of the electric current vector.

On the basis of the above, Formula (11) as a matrix with $\dot{\mathbf{q}} = [\dot{q}_q \ \dot{q}_{cq} \ \dot{\theta}_m]$ can be described in the form of $\mathbf{M}\ddot{\mathbf{q}} + \mathbf{C}\dot{\mathbf{q}} + \mathbf{K}\mathbf{q} = \mathbf{f}$, which makes possible the superimposing of it upon the motion equations of the rigid body system and hydraulic system.

4.2 Validity evaluation of verification model

The verification analysis model consists of Equation (1), which is the motion equation of the rigid body system and hydraulic system, and Equation (11) which represents the electric circuit equation and motion equation of the electric motor. In order to verify the validity of this analysis model, one cycle of the digging operation of the excavator was analyzed and compared with the actual measurement results, in the same manner as in Section 2. In this analysis, the lever input employed was the actual measurement of the operation lever pattern (pilot pressure) of each actuator, and for the slewing speed, the measured speed was employed as the target. As an example, Fig.11 compares the actual measurement results of the cylinder stroke

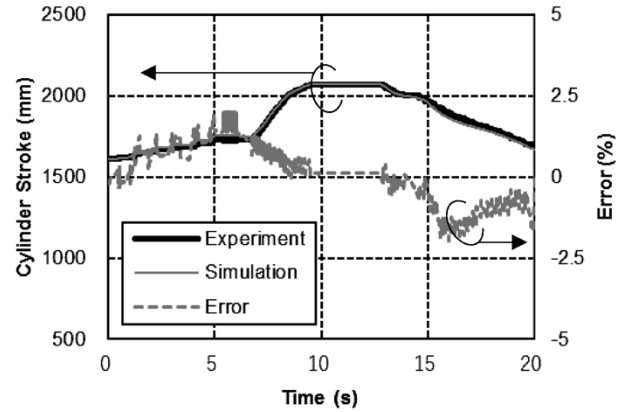


Fig.11 Comparison of experimental and analytical results in digging operation

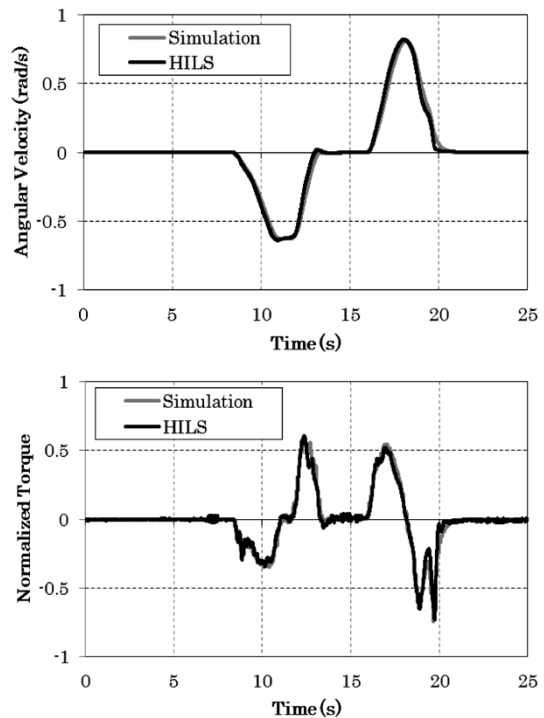


Fig.12 Comparison of responses of HILS system and those of simulation

with the analysis results. They agree with an error of $\pm 2.5\%$ or less, confirming the validity of the verification analysis model.

4.3 HILS evaluation of electric motor during digging operation of hydraulic excavator

The HILS testing for one cycle of the digging operation of the hydraulic excavator was carried out by the electric-motor-load testing apparatus shown in Fig. 8 and Fig. 9 to verify the validity of the electric motor HILS system by comparison with the analysis results of the verification model shown in Subsection 4.2.

Fig.12 shows the slewing angular velocity and

normalized torque obtained by the analysis of the verification model and the HILS testing using the electric-motor-load testing apparatus. These figures confirm that the electric motor HILS system can reproduce the digging operation behaviors with a practically sufficient accuracy.

The following shows that the HILS system developed this time is effective for testing the digging of real machines. First, in the newly developed system, parameters such as the weight of the attachment and the position of the center of gravity of the hydraulic excavator are taken into account in the rigid body system model. In addition, characteristic values such as those of the hydraulic pump and valves are taken into account in the hydraulic system model. As a result, each design parameter can be changed easily in accordance with the change of the evaluation object. Moreover, it is possible to evaluate power that is difficult to measure with actual machines. For example, the evaluation of power loss generated in an electric motor and inverter requires the measurement of the input power and output power for each. Torque meter and power meters are difficult to install on actual equipment; however, they can easily be installed on the HILS system. This enables the detailed evaluation of losses and the designing of energy-saving systems.

Conclusions

This paper has introduced a modeling technique involving the transformation of the motion of a rigid

body system from the motion of a rotating element to the motion of a linear motion element. It has also been shown that a numerical stability more excellent than that of the conventional method is obtained by using this technique in the coupled analysis of a rigid body system and hydraulic system.

In addition, this paper has introduced an electric motor HILS system for the hybrid system, in which both systems are driven by an electric motor, to calculate the load acting on the slewing electric motor in real time, and the results have been reproduced on an electric-motor-load testing apparatus. This system employs an analysis model that can be used for actual design development and is considered to be sufficiently useful as an evaluation tool for hybrid systems.

References

- 1) M. Kagoshima. *R&D Kobe Steel Engineering Reports*. 2012, Vol.62, No.1, pp.14-18.
- 2) Y. Nishida et al. *Komatsu technical report*. 2013, Vol.59, No.166, pp.2-8.
- 3) K. Hagiwara et al. *Transactions of the Society of Automotive Engineers of Japan, Inc.* 2002, Vol.33, No.3, pp.109-114.
- 4) T. Yamaguchi et al. *Transactions of the Japan Society of Mechanical Engineers*, 2013, Vol.79, No.806, pp.3420-3431.
- 5) K. Morita et al. *Transactions of the Japan Society of Mechanical Engineers*, 2014, Vol.80, No.813, p.DR0122.
- 6) K. Morita et al. *Transactions of the Japan Society of Mechanical Engineers*, 2017, Vol.83, No.845, p.16-00234.
- 7) E. Imanishi et al. *Transactions of the Japan Society of Mechanical Engineers*, 1987. Vol.53, No.492, pp.1711-1919.
- 8) Y. Takeda et al. *Umekomi jishaku dōki mōta no sekkei to seigo*. Ohmsha, Ltd. 2010, pp.16-18.